

# Efficient Gating of Magnons by Proximity Superconductors

Tao Yu<sup>1,\*</sup> and Gerrit E. W. Bauer<sup>2,3,4,†</sup>

<sup>1</sup>*School of Physics, Huazhong University of Science and Technology, Wuhan 430074, China*

<sup>2</sup>*WPI-AIMR and Institute for Materials Research and CSRN, Tohoku University, Sendai 980-8577, Japan*

<sup>3</sup>*Zernike Institute for Advanced Materials, University of Groningen, 9747 AG Groningen, Netherlands*

<sup>4</sup>*Kavli Institute for Theoretical Sciences, University of the Chinese Academy of Sciences, Beijing 100190, China*

(Dated: August 10, 2022)

Electrostatic gating confines and controls the transport of electrons in integrated circuits. Magnons, the quanta of spin waves of the magnetic order, are promising alternative information carriers, but difficult to gate. Here we report that superconducting strips on top of thin magnetic films can totally reflect magnons by its diamagnetic response to the magnon stray fields. The induced large frequency shifts unidirectionally block the magnons propagating normal to the magnetization. Two superconducting gates parallel to the magnetization create a magnonic cavity. The option to gate coherent magnons adds functionalities to magnonic devices, such as reprogrammable logical devices and increased couplings to other degrees of freedom.

*Introduction.*—Electrostatic gating provides a tunable potential to control the transport channels of electrons in field effect transistors [1]. Potential barriers size-quantize the electronic wave function, leading to quantum point-contacts, wires, and dots with application in quantum technology [2–4]. “Magnonics” employs the magnon quasiparticles, i.e., the bosonic quanta of the spin wave excitations of the magnetic order, as information carriers in a low-power alternative to conventional electronics [5–14]. However, magnons cannot be gated, blocked, or trapped as easily as electrons, so many mature concepts of electronics cannot directly be applied in magnonics. Chumak *et al.* [15] propose an alternatives to gating in a magnon transistor by inserting a magnonic crystal into a film of yttrium iron garnet (YIG) that controls the transmission of coherent magnons. Current-biased heavy metal contacts can modulate the incoherent magnon currents in a YIG channel by spin injection or heating [16–18]. However, both mechanisms do not create potential barriers, the modulation efficiency is low, and power demands are high. Electrostatic gates on magnetic semiconductors can locally suppress magnetism [19, 20], but at present the magnetic quality of available materials remains wanting.

The dispersion of long-wavelength magnetostatic spin waves in thick films or magnonic crystals can be modulated in a non-reciprocal fashion by the electromagnetic interaction with metallic gates. The latter can be modelled as thick perfect [21] or Ohmic conductors [22–26]. Superconducting gate can have profound effects as well [27–30]. Recent research on ultrathin films accumulates evidence that the physics changes drastically when thicknesses are reduced down to nanometer scale. In this limit surface and volume modes merge into perpendicular standing spin waves (PSSW) with spectra dominated by the exchange interaction. The GHz dynamics is confined to the lowest PSSW with nearly uniform amplitude normal to the film [31–34]. In contrast to conventional wisdom for thick films, a metallic cap atop ultrathin films

of YIG only enhances the damping of spin waves [35, 36] with minor effects on their dispersion. The magnon conductivity in high-quality nanometer films [37] reaches record values because of the onset of two-dimensional diffuse magnon transport. Moreover, stray fields emitted by spin waves in ultrathin films have a relatively short wave length and thereby cannot penetrate deeply into metallic gates, a limit not accounted for by previous theories.

In this Letter, we report that floating superconducting films on top of ultrathin films of a magnetic insulator such as YIG, as illustrated in Fig. 1, induce chiral frequency shifts of tens of GHz that correspond to magnetic fields of  $O(0.1\text{ T})$ . The chirality is caused by constructive interference of the Oersted fields of the spin-wave dipolar and induced eddy currents in the superconductors. The gate generates an effective barrier that is dynamic, i.e., it depends on the magnon frequency and propagation direction. A wide superconducting gate totally reflects coherent magnons in the microwave band propagating normal to the “up” magnetization, but transmits them when magnetization is flipped. We can thereby control the magnon current by either modulating the superconductivity in the gates or rotating the equilibrium magnetization. The on-off ratio is nearly unity over tens of GHz, in contrast to narrow-band resonant coupling effects [38, 39]. Our set-up is exceedingly simple and does not require spin-orbit interactions, in contrast to metal-based designs [40, 41]. Moreover, we predict that two superconducting strips can nearly perfectly trap spin waves in a sub-micrometer region forming a magnon waveguide without having to etch the magnetic film. On-chip implementation of these devices allow to implement magnonic functionalities such as non-volatility and chirality into quantum technologies.

*Inductive interaction between magnons and superconductors.*—We consider a floating superconducting (SC) or normal metal (NM) gate with thickness  $d$  on a thin YIG film of thickness  $s$  as illustrated in Fig. 1. A thin insulating spacer between them suppresses the proximity

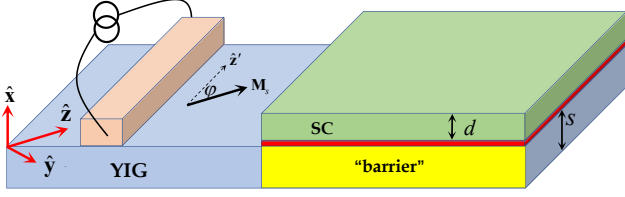


FIG. 1. Unidirectional blocking of magnons by a superconducting metal gate on a thin magnetic insulator that provides an effective “barrier”. An inserted thin insulating layer between the conductors and magnetic films (red) can strongly suppress the interfacial exchange interaction. The stripline on the left acts as injector and detector of coherent magnons. We address reflection as a function of angle of an in-plane magnetic field that rotates the magnetization  $\mathbf{M}_s$ .

effect by an interfacial exchange interaction. We formulate the inductive coupling of propagating magnons under the gate that gives rise to “eddy current” [35, 36, 42]. The magnetization is parallel to and rotates with a weak in-plane applied magnetic field  $\mathbf{H}_{\text{app}}$ , which does not affect the superconductivity. We use a coordinate system in which  $\mathbf{H}_{\text{app}} = H_{\text{app}}\hat{\mathbf{z}}$  and an angle  $\varphi$  relative to the contacts, while the film normal is along  $\hat{\mathbf{x}}$ . We assume that the magnetization dynamics is dominated by isotropic exchange magnons in the thin films and disregard the dipolar interaction on the dispersion and small mode ellipticity as justified in the Supplemental Material [43]. With free boundary conditions [31, 32], the exchange spin waves with amplitudes  $m_y^{(l)}(\mathbf{k}) \approx im_x^{(l)}(\mathbf{k})$  are circularly polarized [43], where  $l$  is the band indices [37, 44].

The dynamic magnetic stray fields emitted by the spin waves induce eddy currents in conductors that in turn generate Oersted magnetic fields  $\mathbf{H}$  that affect the spin-wave dynamics. We focus on metallic gates with  $d \sim O(10 \text{ nm})$  because currents are then constant over the film thickness: London’s penetration depth of SCs  $\lambda_L = \sqrt{m_e/(\mu_0 n_s e^2)} \sim O(100 \text{ nm})$  [45, 46], where  $\mu_0$  is the vacuum permeability and  $m_e$  is the effective mass of electrons with density  $n_s$ . The “skin depth”  $\delta = \sqrt{2/(\mu_0 \omega \sigma_c)}$  of NMs with conductivity  $\sigma_c$  for ac magnetic fields of frequency  $\omega$  [47] is also much larger than  $d$  for good metals at frequencies up to several terahertz (THz). A pioneering study [21] considers “perfectly conducting” gates with  $\sigma_c \rightarrow \infty$  corresponding to  $\delta \rightarrow 0$  and interface boundary condition  $\mathbf{B}_\perp = 0$ , which is very different from the superconductors discussed below.

The dipolar stray fields  $\mathbf{H}_\mathbf{k}^{(l)}(\mathbf{r}, t)$  of spin-wave eigenmodes with momentum  $\mathbf{k}$  and frequency  $\omega_\mathbf{k}$  above the film [43], i.e.,  $\mathbf{r} = (x > 0, \boldsymbol{\rho} = y\hat{\mathbf{y}} + z\hat{\mathbf{z}})$ , are evanescent as  $\sim e^{-|\mathbf{k}|x}$  and nearly uniform across a gate for wave numbers  $|\mathbf{k}| \ll 1/d$  [32]. When  $|\mathbf{k}| \ll 1/s$  only the lowest subband contributes. The components of the magnetic field  $\mathbf{H}_\mathbf{k}^{(l=0)}$  are locked with momentum, obeying  $k_z H_y^{(0)} = k_y H_z^{(0)}$  and  $|\mathbf{k}| H_x^{(0)} = ik_y H_y^{(0)} + ik_z H_z^{(0)}$ .

The stray field vanishes when  $\mathbf{k} = -|k_y|\hat{\mathbf{y}}$ , so spin waves that propagate in the negative  $\hat{\mathbf{y}}$ -direction cannot interact with a top gate.

According to Maxwell’s equations  $\nabla \cdot \mathbf{E} = 0$  and  $\nabla \times \mathbf{E} = i\omega\mu_0\mathbf{H}$ , the magnetic stray field of a spin wave with wavevector  $\mathbf{k}$  and frequency  $\omega$  generates an electromotive force (emf) that has the form  $\mathbf{E} \propto e^{-|\mathbf{k}|x + i\mathbf{k}\cdot\boldsymbol{\rho}}$  up to high frequencies  $\sigma_c/\varepsilon_0 \sim 10^6 \text{ THz}$  for typical metallic conductivities  $\sigma_c \sim 10^7 \Omega^{-1}\text{m}^{-1}$ . The normal component is immediately screened, so  $E_x = 0$ ,  $E_y = -(i\omega\mu_0/|\mathbf{k}|)H_z^{(0)}$ , and  $E_z = (i\omega\mu_0/|\mathbf{k}|)H_y^{(0)}$ . By Ohm’s law, the induced electric eddy current in a normal conductor  $J_x(x, \boldsymbol{\rho}) = 0$ ,  $J_y(x, \boldsymbol{\rho}) = -(i\sigma_c\omega\mu_0/|\mathbf{k}|)H_z^{(0)}(x, \boldsymbol{\rho})$ , and  $J_z(x, \boldsymbol{\rho}) = (i\sigma_c\omega\mu_0/|\mathbf{k}|)H_y^{(0)}(x, \boldsymbol{\rho})$  is perpendicular to the spin-wave propagation direction since  $\mathbf{k} \cdot \mathbf{J} = 0$ . Abrikosov vortice lattices of type-II superconductors are sources of periodic magnetic fields that generate tunable bandgaps in the magnon spectrum [48]. We will address such effects and that of different pairing symmetries in the future.

The eddy currents, in turn, generate Oersted magnetic fields that oppose the original ones (Lenz effect). The effect on the gate itself may be disregarded since we consider only films much thinner than London’s penetration (SC) and skin (NM) depths. However, they affect the spin wave dynamics by a field-like (for SC) or a damping-like (for NM) torque that causes a frequency shift (for SC) and an additional contribution to the Gilbert damping constant (for NM), respectively. Here we address the full dynamic response by self-consistently solving the coupled Maxwell and Landau-Lifshitz-Gilbert (LLG) equations. In the limit that  $|\mathbf{k}| \ll 1/d$ , the currents are uniform across the film and we may set  $x \rightarrow d/2$ . The vector potential generated by the eddy currents then reads in frequency space [47]  $A_\xi(\mathbf{r}, \omega) = (\mu_0/4\pi) \int d\mathbf{r}' J_\xi(x' = d/2, \boldsymbol{\rho}', \omega) e^{i\omega|\mathbf{r}-\mathbf{r}'|/c} / |\mathbf{r}-\mathbf{r}'|$ . Using the Weyl identity [49], we obtain for  $x < 0$

$$A_\xi(\mathbf{r}, \omega) = (\mu_0 d/2) J_\xi(x' = d/2, \boldsymbol{\rho}, \omega) e^{|\mathbf{k}|(x-d/2)/|\mathbf{k}|}. \quad (1)$$

For the LLG equation we require only the transverse ( $x$ - and  $y$ -) components of the Oersted magnetic field  $\tilde{\mathbf{H}}(\mathbf{r}) = \nabla \times \mathbf{A}(\mathbf{r})/\mu_0$ :  $\tilde{H}_y(\mathbf{r}, \omega) = (ik_y/|\mathbf{k}|)\tilde{H}_x(\mathbf{r}, \omega)$  with

$$\begin{aligned} \tilde{H}_x(\mathbf{r}, \omega) &= ie^{|\mathbf{k}|(x-d)} d\sigma_c\omega\mu_0(1 - e^{-|\mathbf{k}|s})/(4|\mathbf{k}|) \\ &\times (m_x^{\mathbf{k}}(\boldsymbol{\rho}, \omega) - im_y^{\mathbf{k}}(\boldsymbol{\rho}, \omega)k_y/|\mathbf{k}|). \end{aligned} \quad (2)$$

The linearized LLG equation in frequency space poses a self-consistency problem

$$\begin{aligned} -i\omega m_x(\mathbf{k}) &= -i\omega_\mathbf{k}(1 - i\alpha_G)m_x(\mathbf{k}) + \mu_0\gamma M_s \tilde{H}_y(\mathbf{k}, \omega), \\ -i\omega m_y(\mathbf{k}) &= -i\omega_\mathbf{k}(1 - i\alpha_G)m_y(\mathbf{k}) - \mu_0\gamma M_s \tilde{H}_x(\mathbf{k}, \omega), \end{aligned}$$

that leads to the modified dispersion relation

$$\tilde{\omega}_\mathbf{k} = \frac{\omega_\mathbf{k}(1 - i\alpha_G)}{1 + i\alpha_m(|\mathbf{k}|)(k_y/|\mathbf{k}| + |k_y|/|\mathbf{k}|)}, \quad (3)$$

where  $\alpha_G$  is the intrinsic Gilbert damping coefficient and

$$\alpha_m(|\mathbf{k}|) = (d/4)e^{|\mathbf{k}|(-\frac{s}{2}-d)}(1 - e^{-|\mathbf{k}|s})\sigma_c\mu_0^2\gamma M_s/|\mathbf{k}| \quad (4)$$

is dimensionless. In the limit that  $|\mathbf{k}| \ll \{1/d, 1/s\}$ ,  $\alpha_m(|\mathbf{k}|) \rightarrow ds\sigma_c\mu_0^2\gamma M_s/4$ . In a normal metal,  $\sigma_c$  is real and  $\alpha_m > 0$ , so only magnons with positive  $k_y$  suffer from an additional damping  $\tilde{\alpha}(\mathbf{k}) = \alpha_m \cos\theta_{\mathbf{k}}(1 + \text{sgn}(k_y))$ , where  $\cos\theta_{\mathbf{k}} = k_y/|\mathbf{k}|$ . For a copper conductor gate with thickness  $d = 40$  nm and conductivity  $\sigma_c \approx 6 \times 10^7 \Omega^{-1}\text{m}^{-1}$  on top of a  $s = 20$  nm thin YIG film with  $\mu_0 M_s = 0.18$  T and  $\gamma = 1.82 \times 10^{11} \text{s}^{-1}\text{T}^{-1}$ , we find  $\alpha_m = 4.8 \times 10^{-4}$ , which is of the same order as the intrinsic damping. Bertelli *et al.* [35] observed a larger  $\alpha_m \sim 10^{-2}$  by nitrogen-vacancy center magnetometry, but for thicker films and only for positive  $\mathbf{k} = |k_y|\hat{\mathbf{y}}$ , therefore did not yet resolve the damping chirality. In contrast to thick films [24], the gate hardly affects the spin wave dispersion Eq. (3).

The chiral damping theory above holds for coherent spin waves with well defined momentum as excited by narrow striplines, and we may expect similar effects in the diffuse regime of magnon transport. An asymmetry in the propagation of carriers into opposite directions has been reported in the transport of incoherent magnons in YIG films under microwave [50] or spin Hall effect [51, 52] excitation. References [51, 52] appear to support our results without having to resort to spin-orbit interactions.

For a superconductor  $\sigma_c(\omega)$  is complex and can be treated by a two-fluid model [53–56]. For simplicity we assume sufficiently low temperatures to freeze out the quasi-particle excitations, but the effect sustains when  $T \rightarrow 0.85T_c$  [43]. The conductivity  $\sigma_c(\tilde{\omega}_{\mathbf{k}}) = in_s e^2 / (m_e \tilde{\omega}_{\mathbf{k}})$  is then purely imaginary, leading to a frequency shift

$$\delta\omega_{\mathbf{k}} = \frac{d}{4} e^{-|\mathbf{k}|(\frac{s}{2}+d)} \frac{1 - e^{-|\mathbf{k}|s}}{|\mathbf{k}|} \mu_0^2 \gamma M_s \frac{n_s e^2}{m_e} \left( \frac{k_y}{|\mathbf{k}|} + \frac{|k_y|}{|\mathbf{k}|} \right), \quad (5)$$

which is real and positive definite. Its chirality is complete since  $\delta\omega_{\mathbf{k}}$  vanishes for negative  $k_y$  and arbitrary  $k_z$ . It is typically quite large: For a  $d = 40$  nm NbN superconducting film with electron density  $n_s = 10^{29}/\text{m}^3$  [57] on top of a  $s = 20$  nm YIG film the shift amounts to  $\delta\omega = 45$  GHz when  $k_y = |\mathbf{k}| \ll \{1/d, 1/s\}$ . This value corresponds to the Zeeman energy of an applied magnetic field of 255 mT. Figure 2 summarizes these features for the chirality of frequency shift [(a)] and spin wave dispersion with momentum  $k_y\hat{\mathbf{y}}$  [(b)]. The singularity in Fig. 2(b) around  $k_y = 0$  has no physical consequences, since the group velocities are positive (negative) for  $k_y > 0$  ( $k_y < 0$ ), but vanishes for Kittel mode at  $k_y = 0$ .

*Unidirectional blocking of magnons.*—The above results imply attractive functionalities created by superconductivity in wave magnonics. A superconducting top gate on a magnetic film forms a nearly perfect switch. It

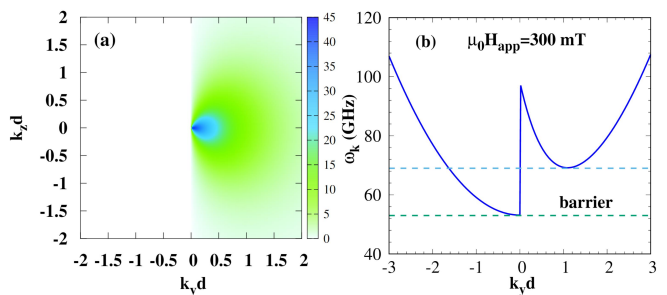


FIG. 2. Chirality of the frequency shift [(a)] and spin wave dispersion with momentum  $k_y\hat{\mathbf{y}}$  [(b)] induced by a superconducting gate. The frequency shift for positive  $k_y$  bars spin wave propagation in a large frequency window of  $\sim 20$  GHz as indicated by the region between the dashed lines in (b). A field  $\mu_0 H_{\text{app}} = 300$  mT is applied in the  $\hat{\mathbf{z}}$ -direction.

is opaque for ballistic spin waves launched, but becomes fully transmitting simply by heating it above the critical superconducting temperature.

The superconducting gate couples most efficiently to spin waves that propagate normal to the magnetization (Damon-Eshbach configuration) as in Fig. 2(b). In order to assess the effect we consider a wide superconducting gate at  $w_1 \leq y \leq w_2$  with width  $w_2 - w_1 \gg \lambda \gg 1/k_y$ , where  $\lambda$  is a magnon relaxation length. It acts as a potential barrier that reflects magnons below an energy threshold just as electric gates in field effect transistors, but now with a  $\mathbf{k}$ -dependent barrier height.

We place a stripline with thickness  $d_s = 80$  nm and width  $w_s = 150$  nm centered at the origin biased by a uniform ac current of frequency  $\nu_s = 2\pi \times \omega_s = 55$  GHz and current density  $I_s = 10^6$  A/cm<sup>2</sup>. When parallel to the external dc field and magnetization in the underlying YIG, it launches spin waves with positive  $k_y^* = 2\pi/0.45 \mu\text{m}^{-1}$  into half space as shown in Fig. 3(a) in the form of a snapshot of the excited magnetization  $|\mathbf{m}|$  [33, 58–61]. The Gilbert damping  $\alpha_G = 10^{-4}$  governs the decay length  $\lambda \sim \sqrt{(\alpha_{\text{ex}}\mu_0\gamma M_s)(\nu_s - \mu_0\gamma H_{\text{app}})/(\alpha_G\nu_s)} = 24.2 \mu\text{m}$ , but it is not a simple exponential since the stripline of finite width also emits waves around  $k_y^*$  that cause the observed interference pattern. A superconducting gate made from a NbN film with thickness  $d = 40$  nm covers the YIG film from  $y = w_1 = 3 \mu\text{m}$  to  $w_2 = 100 \mu\text{m}$ . Below the gate  $w_1 \leq y \leq w_2$ , the diamagnetic field ( $k_y^*d \ll 1, k_y^*s \ll 1$ )

$$\begin{aligned} \tilde{H}_x(y, t) &= -\frac{n_s e^2}{m_e} \mu_0 \frac{ds}{4} \left( m_x(y, t) + \frac{1}{\omega_s} \frac{dm_y(y, t)}{dt} \right), \\ \tilde{H}_y(y, t) &= -\frac{n_s e^2}{m_e} \mu_0 \frac{ds}{4} \left( -\frac{1}{\omega_s} \frac{dm_x(y, t)}{dt} + m_y(y, t) \right), \end{aligned}$$

enters the LLG equation. We solve the time dependent problem in the steady state and show representative  $|\mathbf{m}| \equiv \sqrt{m_x^2 + m_y^2}$  in Fig. 3(b). Technique details are re-

ferred to the Supplemental Material [43]. We clearly observe the total reflection of spin waves at the gate edge due to the excited Oersted field from the superconductor that only exists at its edge [43]. The reflected spin waves penetrate the left half-space in Fig. 3(b), which remains silent in the absence of the gate [Fig. 3(a)] because the pumping is chiral. The amplitude of the magnetization between source and gate  $0 < y < w_1$  is enhanced by a factor 2, i.e., incoming and reflected spin waves interfere constructively. The reflection at the stripline is very weak and cannot generate standing waves in the region  $0 < y < w_1$ . Nevertheless, a large number of coherent emitted and reflected waves with different wave lengths coexist and cause complex interference fringes (refer to Supplemental Material [43] with other parameters). On the other hand, the transmission of spin waves that impinge from the right of the superconducting strip are not affected at all, i.e., the device acts as a spin-wave isolator. Replacing the superconductor by  $d = 40$  nm copper strip, we only enhance the damping of the spin waves without causing reflection [43].

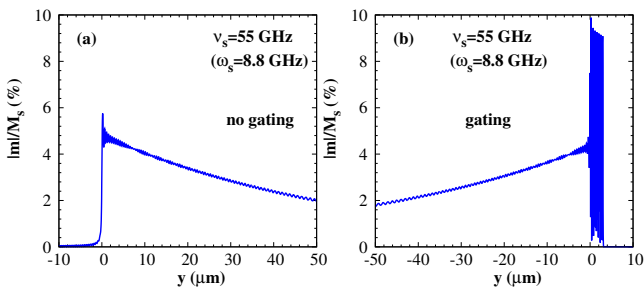


FIG. 3. Excited magnetization  $|\mathbf{m}|$  by a narrow stripline at  $y = 0$  without (a) and with (b) a superconducting gate that covers the region from 3 to 100  $\mu\text{m}$ . The spin waves are totally reflected at the gate edge and leak into the left half space.

*Spin-wave confinement.*—When we rotate the magnetization by  $90^\circ$  to become normal to the gate and stripline, the emitted spin waves  $\mathbf{k} = (0, 0, k_z)$  propagate parallel to the magnetization. The frequency shift of spin waves with positive and negative  $k_z$  under the gates on both sides of the stripline as sketched in Fig. 2(a) are smaller than Damon-Eshbach configuration, but still very substantial. The device therefore forms a cavity, trapping the spin waves analogous to, but without having to nanofabricate, a magnetic film. The standing waves modulate the density of states that are strongly enhanced at the subband edges, which may lead to strong coupling to the stripline photons and other degrees of freedom.

We substantiate these expectations by numerical modelling for a YIG film with two superconducting gates located at  $w_1 \leq |z| \leq w_2$  on both sides of a stripline at the origin as illustrated in Fig. 4(a). The spin waves now feel the back-action magnetic field  $\tilde{H}_x(z, t) = -(n_s e^2 / m_e) \mu_0 d s m_x(z, t) / 4$  and  $\tilde{H}_y(z, t) = 0$ . We self-

consistently solve the LLG equation [43] for cavity widths  $\delta w = 2w_1 = 1$  and  $0.5 \mu\text{m}$  and a stripline frequency interval  $\nu_s \in [53.25, 56]$  GHz indicated in Fig. 4(b), while the other parameters are the same as in Fig. 3. We choose frequencies typical in propagating magnon spectroscopy and stripline widths that can be deposited by state-of-the-art fabrication techniques. The stripline now excites spin waves with equal amplitude to both sides that are reflected by the superconducting gates and interfere. The steady states in Fig. 4(c) are nearly perfectly trapped standing spin waves with odd symmetry. The standing wave resonance for a hard-wall potential are  $\nu_n = \mu_0 \gamma H_{\text{app}} + \alpha_{\text{ex}} \mu_0 \gamma M_s (n\pi / \delta w)^2$ , viz.  $\nu_1 (\delta w = 0.5 \mu\text{m}) = 53.6$  GHz and  $\nu_3 (\delta w = 1 \mu\text{m}) = 54$  GHz. The boundary pinning strongly suppresses the Kittel mode at  $\nu_0 = 53.2$  GHz. The excitation frequency  $\nu_s = 54.5$  GHz is close to the resonances of both cavities.

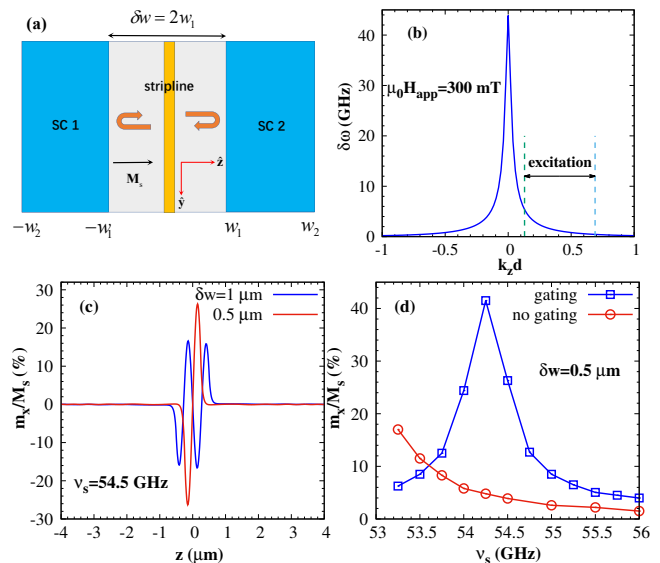


FIG. 4. Spin waves trapped by superconducting gates on both sides of a microwave stripline atop a magnetic thin film magnetized along  $\hat{\mathbf{z}}$ , i.e., normal to the gate. (a) is a top view of the device. (b) shows the frequency shift of magnons under a uniform gate with wave number  $k_z$ . The microwave frequencies in (c) and (d) lie in the window indicated by the vertical dashed lines. In (c), we plot snapshots of the maximum amplitudes  $m_x$  for two gate distances  $\delta w = \{1, 0.5\} \mu\text{m}$  at a frequency close to the standing wave frequencies with index  $n = \{3, 1\}$ . In (d) we plot the excitation efficiencies with and without gating for the  $n = 1$  resonance of the  $0.5 \mu\text{m}$  cavity.

Figure 4(d) illustrates the enhanced excitation efficiency at a standing wave resonance. The maximum at  $\nu_s \sim 54.25$  GHz is not much above the hard-wall estimate of 53.6 GHz, indicating efficient confinement. However, the resonance widths of  $\sim 1$  GHz corresponds to a Gilbert damping of  $\alpha_G = 0.02$  that is much larger than the intrinsic one, indicating substantial gate leakage that can be suppressed by using a thicker superconducting film. Nev-

ertheless, comparison with the ungated result in Fig. 4(d) already shows a cavity enhancement of the magnetization dynamics by an order of magnitude at the resonance.

Microstructuring of YIG films into stripes is usually accompanied by substantial deterioration of the magnetic quality [62]. The trapping of spin waves by superconducting gates only requires deposition of two metal films with a finite gap without introducing additional roughness. Moreover, the option to modulate the trapping offers an easy reprogramming of magnonic logical circuits.

*Discussion and conclusion.*—The predicted total unidirectional reflection is surprising and seems to violate thermodynamic principles. However, we address here a coherent scattering process in a finite system and not a diode-like transport between reservoirs. Furthermore, the physics of chiral reflection of spin waves under a superconducting gate is very different from conventional potential scattering. The reflection of spin waves is a complicated process, in which an approaching wave packet adiabatically generates the diamagnetic current in the superconductor and the associated magnetic fields that push up the magnon gap. The non-equilibrium scattering problem of coherent spin waves injected by an external source that interact with a superconductor gate is not subject to the constraints from linear response.

In conclusion, we predict a non-reciprocal frequency shift of spin waves by the diamagnetism of nearby superconductors, which leads to functionalities such as unidirectional total reflection and confinement of spin waves in magnetic films by top gates. When the gates turn into normal conductors the chiral frequency shift turns into a chiral damping. Both effects enrich the tool box of information communication and processing technology in photonics [49, 63], plasmonics [64–66], acoustics [67, 68], electronics [69, 70], superconductivity [71, 72], and spintronics [73, 74].

This work is financially supported by the startup grant of Huazhong University of Science and Technology (Grants No. 3004012185 and No. 3004012198) as well as JSPS KAKENHI Grant No. 19H00645.

---

\* [taoyuphy@hust.edu.cn](mailto:taoyuphy@hust.edu.cn)

† [G.E.W.Bauer@imr.tohoku.ac.jp](mailto:G.E.W.Bauer@imr.tohoku.ac.jp)

- [1] Y. Imry and R. Landauer, *Rev. Mod. Phys.* **71**, S306 (1999).
- [2] D. Loss and D. P. DiVincenzo, *Phys. Rev. A* **57**, 120 (1998).
- [3] J. Yoneda, K. Takeda, T. Otsuka, T. Nakajima, M. R. Delbecq, G. Allison, T. Honda, T. Kodera, S. Oda, Y. Hoshi, *et al.*, *Nat. Nanotechnol.* **13**, 102 (2018).
- [4] W. Huang, C. H. Yang, K. W. Chan, T. Tanttu, B. Hensen, R. C. C. Leon, M. A. Fogarty, J. C. C. Hwang, F. E. Hudson, K. M. Itoh, *et al.*, *Nature* **569**, 532 (2019).
- [5] B. Lenk, H. Ulrichs, F. Garbs, and M. Muenzenberg, *Phys. Rep.* **507**, 107 (2011).
- [6] A. V. Chumak, V. I. Vasyuchka, A. A. Serga, and B. Hillebrands, *Nat. Phys.* **11**, 453 (2015).
- [7] D. Grundler, *Nat. Nanotechnol.* **11**, 407 (2016).
- [8] V. E. Demidov, S. Urazhdin, G. de Loubens, O. Klein, V. Cros, A. Anane, and S. O. Demokritov, *Phys. Rep.* **673**, 1 (2017).
- [9] A. Brataas, B. van Wees, O. Klein, G. de Loubens, and M. Viret, *Phys. Rep.* **885**, 1 (2020).
- [10] Barman *et al.*, *J. Phys.: Condens. Matter* **33**, 413001 (2021).
- [11] B. Z. Rameshti, S. V. Kusminskiy, J. A. Haigh, K. Usami, D. Lachance-Quirion, Y. Nakamura, C.-M. Hu, H. X. Tang, G. E. W. Bauer, and Y. M. Blanter, *Phys. Rep.* **979**, 1 (2022).
- [12] L. R. Walker, *Phys. Rev.* **105**, 390 (1957).
- [13] R. W. Damon and J. R. Eshbach, *J. Phys. Chem. Solids* **19**, 308 (1961).
- [14] D. D. Stancil and A. Prabhakar, *Spin Waves—Theory and Applications* (Springer, New York, 2009).
- [15] A. V. Chumak, A. A. Serga, and B. Hillebrands, *Nat. Commun.* **5**, 4700 (2014).
- [16] L. J. Cornelissen, J. Liu, B. J. van Wees, and R. A. Duine, *Phys. Rev. Lett.* **120**, 097702 (2018).
- [17] T. Wimmer, M. Althammer, L. Liensberger, N. Vlietstra, S. Geprägs, M. Weiler, R. Gross, and H. Huebl, *Phys. Rev. Lett.* **123**, 257201 (2019).
- [18] J. Liu, X.-Y. Wei, G. E. W. Bauer, J. Ben Youssef, and B. J. van Wees, *Phys. Rev. B* **103**, 214425 (2021).
- [19] F. Matsukura, Y. Tokura, and H. Ohno, *Nat. Nano.* **10**, 209 (2015).
- [20] B. Huang, G. Clark, D. R. Klein, D. MacNeill, E. N.-Moratalla, K. L. Seyler, N. Wilson, M. A. McGuire, D. H. Cobden, D. Xiao, W. Yao, P. J.-Herrero, and X. D. Xu, *Nat. Nano.* **13**, 544 (2018).
- [21] Seshadri, *Proc. IEEE* **58**, 506 (1970).
- [22] M. L. Sokolovskyy, J. W. Klos, S. Mamica, and M. Krawczyk, *J. Appl. Phys.* **111**, 07C515 (2012).
- [23] M. Mruczkiewicz, M. Krawczyk, G. Gubbiotti, S. Tacchi, Y. A. Filimonov, D. V. Kalyabin, I. V. Lisenkov, and S. A. Nikitov, *New J. Phys.* **15**, 113023 (2013).
- [24] M. Mruczkiewicz and M. Krawczyk, *J. Appl. Phys.* **115**, 113909 (2014).
- [25] M. Mruczkiewicz, E. S. Pavlov, S. L. Vysotsky, M. Krawczyk, Y. A. Filimonov, and S. A. Nikitov, *Phys. Rev. B* **90**, 174416 (2014).
- [26] M. Mruczkiewicz, P. Graczyk, P. Lupo, A. Adeyeye, G. Gubbiotti, and M. Krawczyk, *Phys. Rev. B* **96**, 104411 (2017).
- [27] I. A. Golovchanskiy, N. N. Abramov, V. S. Stolyarov, V. V. Bolginov, V. V. Ryazanov, A. A. Golubov, and A. V. Ustinov, *Adv. Funct. Mater.* **28**, 1802375 (2018).
- [28] I. A. Golovchanskiy, N. N. Abramov, V. S. Stolyarov, V. V. Ryazanov, A. A. Golubov, and A. V. Ustinov, *J. Appl. Phys.* **124**, 233903 (2018).
- [29] I. A. Golovchanskiy, N. N. Abramov, V. S. Stolyarov, P. S. Dzhumaev, O. V. Emelyanova, A. A. Golubov, V. V. Ryazanov, and A. V. Ustinov, *Adv. Sci.* **6**, 1900435 (2019).
- [30] I. A. Golovchanskiy, N. N. Abramov, V. S. Stolyarov, A. A. Golubov, V. V. Ryazanov, and A. V. Ustinov, *J. Appl. Phys.* **127**, 093903 (2020).
- [31] C. Bayer, J. Jorzick, B. Hillebrands, S. O. Demokritov, R. Kouba, R. Bozinoski, A. N. Slavin, K. Y. Guslienko,

- D. V. Berkov, N. L. Gorn, and M. P. Kostylev, *Phys. Rev. B* **72**, 064427 (2005).
- [32] T. Yu, C. P. Liu, H. M. Yu, Y. M. Blanter, and G. E. W. Bauer, *Phys. Rev. B* **99**, 134424 (2019).
- [33] T. Yu, Y. M. Blanter, and G. E. W. Bauer, *Phys. Rev. Lett.* **123**, 247202 (2019).
- [34] J. L. Chen, T. Yu, C. P. Liu, T. Liu, M. Madami, K. Shen, J. Y. Zhang, S. Tu, M. S. Alam, K. Xia, M. Z. Wu, G. Gubbiotti, Y. M. Blanter, G. E. W. Bauer, and H. M. Yu, *Phys. Rev. B* **100**, 104427 (2019).
- [35] I. Bertelli, B. G. Simon, T. Yu, J. Aarts, G. E. W. Bauer, Y. M. Blanter, and T. van der Sar, *Adv. Quan. Tech.* **4**, 2100094 (2021).
- [36] S. A. Bunyaev, R. O. Serha, H. Y. Musiienko-Shmarova, A. J. E. Kreil, P. Frey, D. A. Bozhko, V. I. Vasyuchka, R. V. Verba, M. Kostylev, B. Hillebrands, G. N. Kakazei, and A. A. Serga, *Phys. Rev. Applied* **14**, 024094 (2020).
- [37] X. Y. Wei, O. A. Santos, C. H. S. Lusero, G. E. W. Bauer, J. B. Youssef, and B. J. van Wees, arXiv:2112.15165.
- [38] T. Yu, H. C. Wang, M. A. Sentef, H. M. Yu, and G. E. W. Bauer, *Phys. Rev. B* **102**, 054429 (2020).
- [39] K. G. Fripp, A. V. Shytov, and V. V. Kruglyak, *Phys. Rev. B* **104**, 054437 (2021).
- [40] J. Lan, W. C. Yu, R. Q. Wu, and J. Xiao, *Phys. Rev. X* **5**, 041049 (2015).
- [41] K. Szulc, P. Graczyk, M. Mruczkiewicz, G. Gubbiotti, and M. Krawczyk, *Phys. Rev. Applied* **14**, 034063 (2020).
- [42] M. A. Schoen, J. M. Shaw, H. T. Nembach, M. Weiler, and T. J. Silva, *Phys. Rev. B* **92**, 184417 (2015).
- [43] See Supplemental Material at [...] for the justification of the role of dipolar interaction, derivation of PSSW, and numerical details for the gated magnetization dynamics.
- [44] T. Yu, C. Wang, M. A. Sentef, and G. E. W. Bauer, *Phys. Rev. Lett.* **126**, 137202 (2021).
- [45] J. R. Schrieffer, *Theory of Superconductivity* (W. A. Benjamin, New York, 1964).
- [46] C. Kittel, *Introduction to Solid State Physics*, 5th. ed. (Wiley, New York, 1976).
- [47] J. D. Jackson, *Classical Electrodynamics* (Wiley, New York, 1998).
- [48] O. V. Dobrovolskiy, R. Sachser, T. Brächer, T. Böttcher, V. V. Kruglyak, R. V. Vovk, V. A. Shklovskij, M. Huth, B. Hillebrands, and A. V. Chumak, *Nat. Phys.* **15**, 477 (2019).
- [49] L. Novotny and B. Hecht, *Principles of Nano-Optics* (Cambridge University Press, Cambridge, England, 2006).
- [50] J. Liu, F. Feringa, B. Flebus, L. J. Cornelissen, J. C. Leutenantsmeyer, R. A. Duine, and B. J. van Wees, *Phys. Rev. B* **99**, 054420 (2019).
- [51] R. Schlitz, S. Vélez, A. Kamra, C.-H. Lambert, M. Lamme, S. T. B. Goennenwein, and P. Gambardella, *Phys. Rev. Lett.* **126**, 257201 (2021).
- [52] J. H. Han, Y. B. Fan, B. C. McGoldrick, J. Finley, J. T. Hou, P. X. Zhang, and L. Q. Liu, *Nano Lett.* **21**, 7037 (2021).
- [53] R. A. Kaindl, M. A. Carnahan, J. Orenstein, D. S. Chemla, H. M. Christen, H. Y. Zhai, M. Paranthaman, and D. H. Lowndes, *Phys. Rev. Lett.* **88**, 027003 (2001).
- [54] J. Demsar, R. D. Averitt, A. J. Taylor, V. V. Kabanov, W. N. Kang, H. J. Kim, E. M. Choi, and S. I. Lee, *Phys. Rev. Lett.* **91**, 267002 (2003).
- [55] R. A. Kaindl, M. A. Carnahan, D. S. Chemla, S. Oh, and J. N. Eckstein, *Phys. Rev. B* **72**, 060510(R) (2005).
- [56] T. Yu and M. W. Wu, *Phys. Rev. B* **96**, 155311 (2017).
- [57] S. P. Chockalingam, M. Chand, J. Jesudasan, V. Tripathi, and P. Raychaudhuri, *Phys. Rev. B* **77**, 214503 (2008).
- [58] I. Bertelli, J. Carmiggelt, T. Yu, B. G. Simon, C. C. Pothoven, G. E. W. Bauer, Y. M. Blanter, J. Aarts, and T. van der Sar, *Sci. Adv.* **6**, eabd3556 (2020).
- [59] T. Schneider, A. A. Serga, T. Neumann, B. Hillebrands, and M. P. Kostylev, *Phys. Rev. B* **77**, 214411 (2008).
- [60] V. E. Demidov, M. P. Kostylev, K. Rott, P. Krzyszczyk, G. Reiss, and S. O. Demokritov, *Appl. Phys. Lett.*, **95**, 112509 (2009).
- [61] T. Yu, Z. Luo, and G. E. W. Bauer, arXiv:2206.05535.
- [62] Q. Wang, B. Heinz, R. Verba, M. Kewenig, P. Pirro, M. Schneider, T. Meyer, B. Lägél, C. Dubs, T. Brächer, and A. V. Chumak, *Phys. Rev. Lett.* **122**, 247202 (2019).
- [63] P. Lodahl, S. Mahmoodian, S. Stobbe, A. Rauschenbeutel, P. Schneeweiss, J. Volz, H. Pichler, and P. Zoller, *Nature (London)* **541**, 473 (2017).
- [64] F. J. Rodríguez-Fortuño, G. Marino, P. Ginzburg, D. O'Connor, A. Martínez, G. A. Wurtz, and A. V. Zayats, *Science* **340**, 328 (2013).
- [65] K. Y. Bliokh, D. Smirnova, and F. Nori, *Science* **348**, 1448 (2015).
- [66] K. Y. Bliokh and F. Nori, *Phys. Rep.* **592**, 1 (2015).
- [67] H. Nassar, B. Yousefzadeh, R. Fleury, M. Ruzzene, A. Alú, C. Daraio, A. N. Norris, G. Huang, and M. R. Haberman, *Nat. Rev. Mat.* **5**, 667 (2020).
- [68] C. Rasmussen, L. Quan, and A. Alú, *J. Appl. Phys.* **129**, 210903 (2021).
- [69] N. Reiskarimian and H. Krishnaswamy, *Nat. Commun.* **7**, 11217 (2016).
- [70] A. Nagulu, N. Reiskarimian, and H. Krishnaswamy, *Nat. Electro* **3**, 241 (2020).
- [71] F. Ando, Y. Miyasaka, T. Li, J. Ishizuka, T. Arakawa, Y. Shiota, T. Moriyama, Y. Yanase, and T. Ono, *Nature* **584**, 373 (2020).
- [72] Y. M. Itahashi, T. Ideue, Y. Saito, S. Shimizu, T. Ouchi, T. Nojima, and Y. Iwasa, *Sci. Adv.* **6**, eaay9120 (2020).
- [73] S.-H. Yang, *Appl. Phys. Lett.* **116**, 120502 (2020).
- [74] S.-H. Yang, R. Naaman, Y. Paltiel, and S. S. P. Parkin, *Nat. Rev. Phys.* **3**, 328 (2021).